

Effective Hamiltonian for an off-resonantly driven qubit-cavity system

Downloaded from: https://research.chalmers.se, 2026-11-29 01:29 UTC

Citation for the original published paper (version of record):
Jirlow, M., Helambe, K., Eriksson Lundström, A. et al (2026). Effective Hamiltonian for an off-resonantly driven qubit-cavity system. Physical Review A, 114(4).
http://dx.doi.org/10.1103/y7xr-jq5w

N.B. When citing this work, cite the original published paper.

research.chalmers.se offers the possibility of retrieving research publications produced at Chalmers University of Technology. It covers all kind of research output: articles, dissertations, conference papers, reports etc. since 2004. research.chalmers.se is administrated and maintained by Chalmers Library

(article starts on next page)

Effective Hamiltonian for an off-resonantly driven qubit-cavity system

Martin Jirlow,* Kunal Helambe, Axel M. Eriksson, Simone Gasparinetti, and Tahereh Abad†
Department of Microtechnology and Nanoscience, Chalmers University of Technology, 412 96 Gothenburg, Sweden

(Received 8 October 2025; revised 1 April 2026; accepted 2 September 2026; published 6 October 2026)

Accurate modeling of driven light-matter interactions is essential for quantum technologies, where natural and synthetic atoms are used to store and process quantum information, mediate interactions between bosonic modes, and enable nonlinear operations. In systems subject to multitone drives, however, the theoretical description becomes challenging and existing models cannot quantitatively reproduce the experimental data. Here, we derive an effective Hamiltonian that retains slowly rotating terms, providing a general framework for accurately describing driven dynamics across platforms. As a concrete application, we validate the theory in circuit QED, where it quantitatively reproduces experimentally measured ac Stark shifts and captures key interactions such as two-mode squeezing and beam splitting. Our results establish a broadly applicable tool to engineer driven interactions in quantum information processing platforms.

DOI: 10.1103/y7xr-jq5w

I. INTRODUCTION

Accurate control of driven light-matter interactions is central to quantum technologies, where natural and synthetic atoms coupled to bosonic modes enable information storage, processing, mediated interactions, and nonlinear operations in platforms from circuit quantum electrodynamics (QED) [1–3] to trapped ions [4–6] and optomechanics [7,8]. A standard route to controlling bosonic modes is to couple them dispersively to an ancillary nonlinear element such as a qubit. The resulting photon-number-dependent frequency shifts enable selective addressing of Fock states [9–11], forming the basis of universal bosonic control. In practice, realizing nonlinear interactions often requires multitone off-resonant driving of the coupled system [11–15]. While experimentally effective, such driving is theoretically challenging: conventional displaced-frame treatments [14,16] combined with rotating-wave approximations (RWAs) break down in the near-resonant regime [15]. A particularly striking failure is their inability to reproduce the measured Stark shift of the qubit.

Here, we present an effective Hamiltonian framework that extends the displaced-frame approach by retaining near-resonant contributions. The method applies broadly; similar displacement-based approaches have also been explored in optomechanical platforms [17–19], trapped ions [20], and atomic ensembles [21]. As a concrete application, we focus here on circuit QED in the strong dispersive regime [22–28]. We validate the model against experimental data from Ref. [15], where it quantitatively reproduces ac Stark shifts and accurately captures driven interactions such as two-mode squeezing, as well as against beam-splitting measurements performed in the present work. Our results show that standard approximations can fail even qualitatively in regimes used in current experiments, and provide a predictive, quantitatively accurate framework for designing driven quantum interactions in anharmonic platforms. To facilitate reproducibility and further exploration, the source code implementing the effective Hamiltonian framework is available at Ref. [29].

II. SYSTEM HAMILTONIAN

We consider a driven system comprising a transmon-type qubit dispersively coupled to a cavity, described by the Hamiltonian [30]

$$H = H_{\text{free}} + H_{\text{drive}}, \tag{1}$$

where

$$H_{\text{free}} = \omega_c a^\dagger a + \omega_q b^\dagger b - \frac{E_J}{24}[\varphi_q(b+b^\dagger) + \varphi_c(a+a^\dagger)]^4, \tag{2}$$

describes a bosonic cavity mode a coupled to a transmon qubit mode b. Here, ω_c and ω_q are the renormalized mode frequencies, E_J is the Josephson energy, and φ_c, φ_q are the dimensionless zero-point flux fluctuations across the junction.

The system is driven by N tones on the cavity and M tones on the qubit, with drive Hamiltonian

$$H_{\text{drive}} = \sum_{n=1}^{N} \varepsilon_c^{(n)} \cos\left(\omega_{cd}^{(n)} t + \theta_c^{(n)}\right) a^\dagger + \sum_{n=1}^{M} \varepsilon_q^{(n)} \cos\left(\omega_{qd}^{(n)} t + \theta_q^{(n)}\right) b^\dagger + \text{H.c.}, \tag{3}$$

*Contact author: martin.jirlow@chalmers.se
†Contact author: tahereh.abad@chalmers.se

Published by the American Physical Society under the terms of the Creative Commons Attribution 4.0 International license. Further distribution of this work must maintain attribution to the author(s) and the published article's title, journal citation, and DOI. Funded by Bibsam.

where $\varepsilon_i^{(n)}$ and $\theta_i^{(n)}$ are the amplitude and phase of the nth drive on mode $i = q, c$. Avoiding the conventional approximation $a^\dagger e^{-i\omega t} + \text{H.c.}$, we retain the full cosine form, which contains both positive- and negative-frequency components. In a rotating frame at the drive frequency, one component becomes stationary while the other is usually discarded as rapidly oscillating. As we show below, however, this counterrotating contribution can combine with off-diagonal terms of the system Hamiltonian and generate effective resonant processes, making it essential to keep both.

Each drive frequency can be expressed in terms of its detuning from the corresponding mode frequency,

$$\omega_{id}^{(n)} = \omega_i + \Delta_i^{(n)}, \quad \text{for } i = q, c, \tag{4}$$

with detuning $\Delta_i^{(n)}$ from the mode frequency ω_i.

Moving to a rotating frame at the cavity and qubit frequencies, and applying the RWA, the diagonal part of Eq. (2) becomes

$$H_{\text{free}}^{\text{diag}} = -\frac{\alpha}{2} b^{\dagger 2} b^2 - \frac{K_c}{2} a^{\dagger 2} a^2 - \chi b^\dagger b a^\dagger a, \tag{5}$$

where α is the qubit anharmonicity, K_c the cavity Kerr, and χ the dispersive coupling. In the absence of drives, rapidly rotating terms beyond Eq. (5) average out and can be neglected. In the presence of driving, however, these terms can combine with counterrotating components of the drives Eq. (3), cancel their oscillations, and become effectively resonant in the displaced frame. As a result, contributions such as $b^{\dagger 3} b$ that rotate at $2\omega_q$ must be retained to capture the correct dynamics. In the next section, we show how these contributions enter the effective Hamiltonian.

III. EFFECTIVE MODEL

In the conventional displaced-frame treatment, one obtains an effective Hamiltonian by applying a displacement transformation that removes the linear drive terms, followed immediately by the RWA. For clarity, we will refer to this scheme as the "Early RWA" approach, since the RWA is applied at an early stage of the derivation. This procedure exposes higher-order interactions from the transmon nonlinearity, such as $a^\dagger b^\dagger$ enabling two-excitation processes [14,15], $ab^\dagger$ corresponding to excitation exchange [33], or four-wave mixing interaction [34].

In our approach, we first move into a frame rotating at the cavity and qubit frequencies, and then apply the displacement transformation. This allows certain counterrotating contributions of the drive to survive in the displaced frame, which play a key role in the driven dynamics [30]. We then apply the RWA only at the final step, an approach we call "Late RWA," which ensures that slowly rotating contributions at small detunings (such as the $b^{\dagger 2} b$ term) are retained. The displacement transformation is implemented by the unitary

$$U(t) = D_q[\xi_q(t)] D_c[\xi_c(t)], \tag{6}$$

where D_q and D_c are displacement operators for the qubit and cavity modes. The displacement amplitudes $\xi_q(t)$ and $\xi_c(t)$ are chosen to cancel the linear drive terms of Eq. (3) and decompose into contributions from both co- and counterrotating drive components,

$$\xi_i(t) = \sum_{n=1}^{N_i} \left[\xi_{i,1}^{(n)}(t) + \xi_{i,2}^{(n)}(t) e^{i 2\omega_i t} \right], \quad \text{for } i = q, c, \tag{7}$$

where the second term originates from the counterrotating part of the cosine drives. The explicit forms of $\xi_{i,1}^{(n)}$ and $\xi_{i,2}^{(n)}$ are given by [30]

$$\begin{aligned} \xi_{i,1}^{(n)}(t) &= \frac{\varepsilon_i^{(n)} e^{-i\theta_i^{(n)}}}{-2\Delta_i^{(n)} - i\kappa_i} e^{-i\Delta_i^{(n)} t}, \\ \xi_{i,2}^{(n)}(t) &= \frac{\varepsilon_i^{(n)} e^{i\theta_i^{(n)}}}{4\omega_i + 2\Delta_i^{(n)} - i\kappa_i} e^{i\Delta_i^{(n)} t}, \end{aligned} \quad \text{for } i = q, c, \tag{8}$$

where κ_q and κ_c are the qubit and cavity decay rates. Including these rates ensures consistency with the Lindblad master equation, since the inhomogeneous transformation that defines the displacement must leave the dissipators invariant [30]. In the limit $\Delta_i^{(n)} \gg \kappa_i$, their contribution becomes negligible. For compactness, we write $\xi_{i,1}$ and $\xi_{i,2}$ as shorthand for the sums $\xi_{i,1}(t) = \sum_{n=1}^{N_i} \xi_{i,1}^{(n)}(t)$ and $\xi_{i,2}(t) = \sum_{n=1}^{N_i} \xi_{i,2}^{(n)}(t)$, respectively, with $i = q, c$. For brevity, we omit the explicit time dependence of these terms in what follows.

Under the assumption that the drive detunings are small enough to avoid superharmonic processes such as $b^{\dagger 3} + \text{H.c.}$, we apply Eq. (6) to the total Hamiltonian Eq. (1) in the rotating frame and, after performing the RWA, obtain the effective Hamiltonian [30]

$$H_{\text{eff}} = H_{\text{diag}} + H_1 + H_2. \tag{9}$$

Here, H_{diag} presents the diagonal part

$$H_{\text{diag}} = \delta_q b^\dagger b + \delta_c a^\dagger a - \frac{\alpha}{2} b^{\dagger 2} b^2 - \frac{K_c}{2} a^{\dagger 2} a^2 - \chi b^\dagger b a^\dagger a, \tag{10}$$

with drive-induced shifts $\delta_q = -2\alpha|\xi_{q,1}|^2 - \chi|\xi_{c,1}|^2$ and $\delta_c = -2K_c|\xi_{c,1}|^2 - \chi|\xi_{q,1}|^2$. These terms correspond to the ac Stark shifts obtained in the Early RWA treatment, but that approximation fails to reproduce the experimentally observed shifts.

The interaction part H_1 arises from the displacement of anharmonic and dispersive terms, and takes the form

$$\begin{aligned} H_1 = &-\frac{\alpha}{2}\left(\xi_{q,1}^2 b^{\dagger 2} - 2\xi_{q,1} b^{\dagger 2} b\right) - \frac{K_c}{2}\left(\xi_{c,1}^2 a^{\dagger 2} - 2\xi_{c,1} a^{\dagger 2} a\right) \\ &- \chi(\xi_{q,1}\xi_{c,1} b^\dagger a^\dagger + \xi_{q,1}^* \xi_{c,1} b a^\dagger - \xi_{c,1} b^\dagger b a^\dagger - \xi_{q,1} b^\dagger a^\dagger a) \\ &+ (\alpha \xi_{q,1}|\xi_{q,1}|^2 + \chi \xi_{q,1}|\xi_{c,1}|^2) b^\dagger \\ &+ (K_c \xi_{c,1}|\xi_{c,1}|^2 + \chi \xi_{c,1}|\xi_{q,1}|^2) a^\dagger + \text{H.c.} \end{aligned} \tag{11}$$

Here, we see, for example, that making the two-photon term $b^\dagger a^\dagger$ resonant requires canceling the time dependence in $\xi_{q,1}\xi_{c,1}$, which is achieved by choosing opposite detunings, $\Delta_c^{(n)} = -\Delta_q^{(n)} = \Delta$ in Eq. (8). The remaining terms then rotate at frequencies that are integer multiples of Δ. When $1/\Delta$ is similar to or larger than the dynamical timescale, these terms remain slowly varying and contribute significantly to the system evolution. In Ref. [35], only the cavities are displaced, which does not capture the effects of off-resonant qubit driving.

Finally, H_2 contains contributions from counterrotating drive terms, including terms oscillating at $2\omega_q$, $2\omega_c$ in the

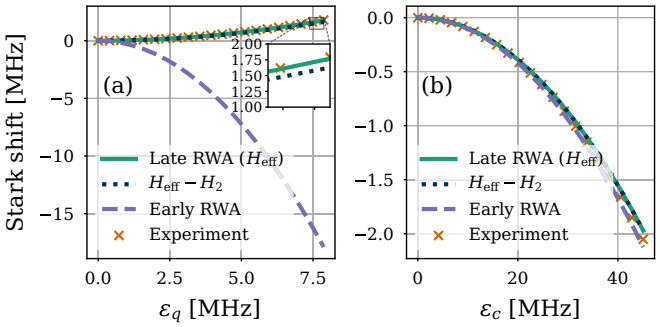

FIG. 1. Ac Stark shift of the qubit frequency under (a) a qubit drive at $\omega_q + \Delta_q$ ($\Delta_q = -20$ MHz) and (b) a cavity drive at $\omega_c + \Delta_c$ ($\Delta_c = 18.5$ MHz), as functions of drive amplitudes ε_q and ε_c, respectively. Simulations using H_{eff} obtained from the Late RWA method show excellent agreement with experimental data, while Early RWA fails to reproduce the correct sign and magnitude in (a). The inset in (a) highlights the noticeable contribution of the correction H_2.

rotating frame, or higher-order mixing frequencies. These become relevant through the time dependence of $\xi_{i,2}$:

$$H_2 = \alpha\xi^*_{q,2}b^{\dagger 2}b - K_c\xi^*_{c,2}a^{\dagger 2}a - \frac{\chi}{6}(\xi^*_{q,2}\xi^*_{c,2}b^\dagger a^\dagger + \xi_{q,2}\xi^*_{c,2}ba^\dagger) + \frac{\chi}{6}(\xi^*_{c,2}b^\dagger ba^\dagger + \xi^*_{q,2}b^\dagger a^\dagger a) + \text{H.c.} \quad (12)$$

The counterrotating contribution Eq. (12) provides a small but non-negligible correction to Eq. (11). It originates from rapidly oscillating terms in the Josephson cosine expansion whose rotation is canceled by the counterrotating components of the drive fields.

Equations (9)–(12) constitute *the main result* of this article: an effective Hamiltonian describing the dynamics of a cavity-qubit system under off-resonant multitone driving, including frequency shifts, induced interactions, and counterrotating corrections.

IV. MODEL VALIDATION

We validate the effective Hamiltonian Eq. (9) by comparing its predictions for the qubit ac Stark shift in the coupled qubit-cavity system with experimental data. Single-tone drives are applied either to the qubit or the cavity: the qubit is driven red-detuned at $\omega_q + \Delta_q$ ($\Delta_q < 0$), and the cavity blue-detuned at $\omega_c + \Delta_c$ ($\Delta_c > 0$), with the specific detunings given in the caption of Fig. 1. Simulations use the parameters of Ref. [15].

The Stark shift is defined as the change in the dressed qubit frequency extracted from the spectrum of H_{eff} Eq. (9) relative to its undriven value. For single-tone drives, H_{eff} can be made time independent by moving into an additional rotating frame at the detuning Δ_i. Since we are already in the frame rotating at ω_i, this extra transformation effectively brings us into the interaction picture at the drive frequency $\omega_i + \Delta_i$. In this frame, the phase rotation of $\xi_{i,j}$ ($i = q, c$, $j = 1, 2$) is canceled, yielding well-defined eigenstates and eigenenergies. Figure 1(a) shows the shift under qubit driving, with excellent agreement between model and experiment to within ∼20 kHz (1.3% error). Figure 1(b) shows the cavity-drive case, with

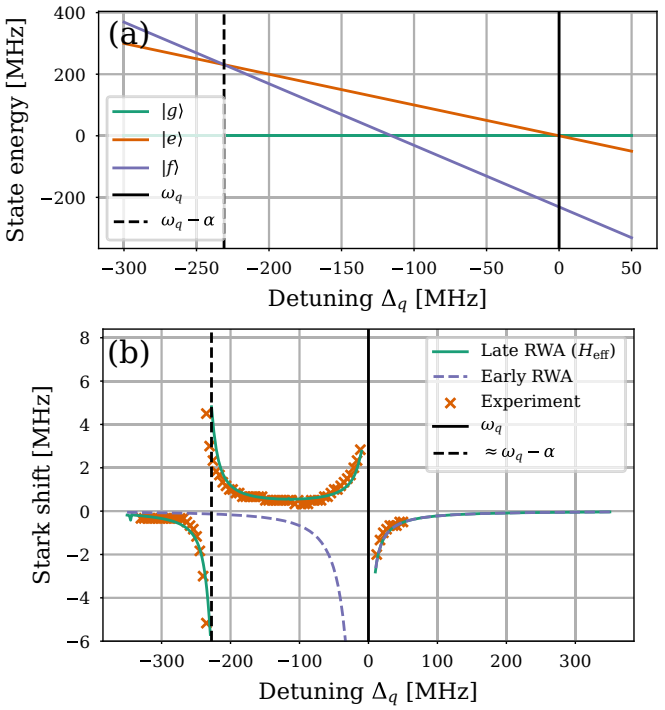

FIG. 2. (a) Qubit state energies for the states $|g\rangle$, $|e\rangle$, and $|f\rangle$ in a frame rotating at the drive frequency. (b) Qubit Stark shift vs detuning for a fixed qubit drive amplitude $\varepsilon_q = 7.63$ MHz. The Late RWA approach (H_{eff}) captures both the sign change across resonance and the transition near $\Delta_q \approx -\alpha$, features that are missed by the Early RWA method. The system parameters are listed in Table S1 [30].

deviations below ∼81 kHz (3.9% error). Importantly, the effective Hamiltonian obtained from the Late RWA approach reproduces both the *magnitude and sign* of the shift, unlike the Early RWA which predicts a negative shift. The correction H_2, although small, makes a visible difference in Fig. 1(a).

To understand this discrepancy for $\Delta_q < 0$, note that earlier models neglect terms rotating at frequencies $\sim\Delta_q$, which is only valid when $|\Delta_q|$ is large [33]. At small detuning, these terms rotate slowly and crucially affect the Stark shift. Figure 2(b) shows the Stark shift versus detuning, revealing a sign change across resonance and a critical transition around $\Delta_q \approx -\alpha$, due to an avoided level crossing between the $|e\rangle_q$ and $|f\rangle_q$ qubit states in the rotating frame, where the three lowest-energy eigenstates of the qubit are denoted $|g\rangle_q$, $|e\rangle_q$, and $|f\rangle_q$. This difference originates from the treatment of the slowly rotating coupling terms responsible for the avoided-level repulsion: the Late RWA retains these terms, while the Early RWA discards them. Consequently, only the Late RWA captures the resulting modification of the dressed-state spectrum. The Early RWA instead retains only the drive-induced self-Kerr contribution from δ_q in H_{diag}.

This is especially relevant for $\Delta_q \in (-\alpha, 0)$, where the dressed state $|e\rangle_q$ lies energetically above $|g\rangle_q$ and $|f\rangle_q$ in the rotating frame. This can be seen in Fig. 2(a). Driven repulsion from both neighboring levels therefore shifts the energy of $|e\rangle_q$ upward, and this positive contribution outweighs the negative shift from δ_q. The net result is a positive Stark shift.

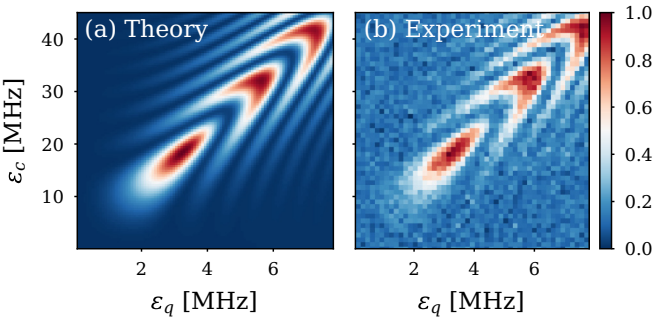

FIG. 3. Qubit population under the two-mode squeezing transition $|0\rangle_c |g\rangle_q \rightarrow |1\rangle_c |e\rangle_q$, as a function of drive amplitudes ε_q and ε_c, after a gate time $\tau = 4.2$ μs. (a) Simulation using the effective Hamiltonian Eq. (9). (b) Experimental data from Ref. [15].

This repulsion mechanism is absent in the Early RWA, which fails to reproduce the experimentally observed sign change. This feature, consistent with experiment, is beyond the reach of previous approximations [14,15]. Finally, the model also captures the Stark shift of the cavity induced by qubit driving (see Supplemental Material [30]), which is much smaller (∼50 kHz) due to the cavity's near-harmonic spectrum.

We now demonstrate the utility of our effective Hamiltonian by analyzing two fundamental interactions that arise when driving both the qubit and cavity with two tones: two-mode squeezing and beam splitting.

A. Two-mode squeezing

This regime involves two-photon creation processes of the form $a^\dagger b^\dagger$, enabling entanglement generation between the qubit and cavity modes [14,15]. A notable example is the selective number-dependent arbitrary-phase photon-addition (SNAPPA) protocol [15], which employs off-resonant drives to realize number-selective interactions. In SNAPPA, a single-qubit drive at $\Delta_q = -\Delta$ is combined with a multitone cavity drive at $\Delta_c^{(n)} = \Delta - (n+1)\chi$, where n spans the photon numbers from a chosen parity subspace (e.g., all odd n), χ is the dispersive shift, and Δ is a small detuning on the order of tens of MHz. These drives coherently induce transitions $|n\rangle_c |g\rangle_q \rightarrow |n+1\rangle_c |e\rangle_q$, thereby adding a photon conditioned on photon number parity, while simultaneously exciting the qubit and imprinting a programmable phase dependent on the relative phases of the drive fields. Such number- and parity-selective operations are key resources for bosonic error correction [13,15].

We simulate H_{eff}, Eq. (9), using the system parameters as in Ref. [15], with single-tone drives on the qubit and cavity at amplitudes ε_q and ε_c. Drive frequencies are chosen to implement the SNAPPA transition $|0\rangle_c |g\rangle_q \rightarrow |1\rangle_c |e\rangle_q$ (i.e., $n = 0$). Figure 3(a) shows the simulated qubit population, as ε_q and ε_c are varied. The resulting interference pattern closely matches the experimental data in Fig. 3(b), confirming that Late RWA captures the relevant dynamics. Additional simulations in the Supplemental Material [30] show qubit populations for higher-order two-mode squeezing transitions, where H_{eff} reproduces the experimental chevrons while the Early RWA model shows clear discrepancies.

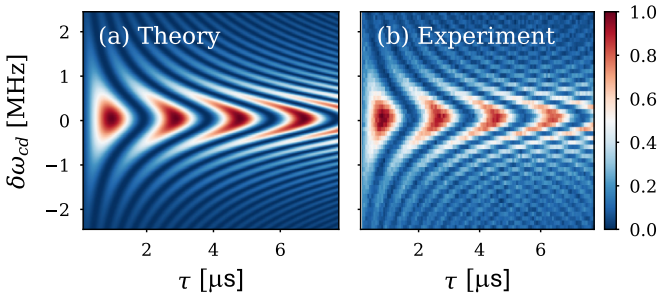

FIG. 4. Qubit population under the beam-splitting transition $|1\rangle_c |g\rangle_q \leftrightarrow |0\rangle_c |e\rangle_q$, as a function of gate time τ and cavity drive frequency offset $\delta\omega_{cd}$. The drive frequencies are $\omega_{qd} = \omega_q + \Delta_q$ and $\omega_{cd} = \omega_c + \Delta_c + \nu_{\text{corr}} + \delta\omega_{cd}$, with $\Delta_q = \Delta_c = -50$ MHz and $\nu_{\text{corr}} \approx -5.02$ MHz, an experimental correction that centers the pattern. (a) Simulation using the effective Hamiltonian Eq. (9). (b) Experimental data, taken with the parameters of Table S1 in Supplemental Material [30].

B. Beam-splitting interaction

This regime corresponds to another two-photon process in which an excitation is swapped between the qubit and cavity modes, and is commonly used to implement controlled SWAP gates [14,33,36]. It can be driven using a qubit and cavity tone with matched detunings, $\Delta_q = \Delta_c = \Delta$, such that $\omega_{qd} - \omega_{cd} = \omega_q - \omega_c$. This condition selectively drives the conversion $|n\rangle_c |e\rangle_q \leftrightarrow |n+1\rangle_c |g\rangle_q$. Figure 4(a) shows the simulated qubit population for the beam-splitting transition, starting from the initial state $|1\rangle_c |g\rangle_q$, as a function of gate time τ and cavity drive frequency offset $\delta\omega_{cd}$. The drives are set with $\Delta = -50$ MHz, and $\omega_{cd} = \omega_c + \Delta + \nu_{\text{corr}} + \delta\omega_{cd}$, where $\nu_{\text{corr}} \approx -5.02$ MHz is an experimental correction that centers the beam-splitting pattern. The simulation uses the system parameters listed in Table S1 of the Supplemental Material [30]. The simulated dynamics closely match the experimental data in Fig. 4(b), demonstrating that the effective Hamiltonian provides an accurate description of the beam-splitting interaction.

V. OUTLOOK

We derived an effective Hamiltonian for a driven cavity-transmon system that goes beyond the conventional displaced-frame treatments. Beyond resolving a theoretical inconsistency, this framework provides a predictive tool for designing and calibrating driven quantum operations, reducing the need for empirical tuning and enabling more reliable control of bosonic modes. Given its generality across anharmonic platforms, this approach has immediate implications for high-fidelity gate design [10,12,14,37], bosonic error correction [13,15,38,39], and Hamiltonian engineering in a wide range of quantum technologies [40,41].

In this approach, which we refer to as the Late RWA method, the RWA is applied only after transforming into a rotating frame and performing the displacement. In contrast to the conventional Early RWA method, where the RWA is applied immediately after displacement, deferring the approximation preserves counterrotating drive contributions

in the displaced frame. The model applies to off-resonant multitone driving, with particular importance in the near-resonant regime, where the Early RWA method fails. It reproduces experimental features, such as the qubit and cavity ac Stark shifts, and accurately captures beam-splitting and two-photon processes.

This framework enables predictive simulation of systems under arbitrary multitone driving on both qubit and cavity, allowing precise evaluation of cumulative Stark effects from complex drive spectra. Such capability is particularly valuable for high-fidelity control, where even small, Fock-dependent shifts, especially in the cavity, can be used to sculpt the transition landscape and mitigate unwanted nonlinearities [42,43]. While we focused here on the fundamental transmon transition, the same approach naturally extends to any anharmonic oscillator, including other qubit types such as the fluxonium [44–47], phase [48], and flux qubits [49–51].

Looking forward, extending the method to include superharmonic processes could open the door to modeling higher-order transitions such as $|0\rangle_c |f\rangle_q \leftrightarrow |1\rangle_c |g\rangle_q$ [52], and to applications ranging from dissipation engineering via lossy buffer modes [13] to on-demand microwave photon generation in parametrically driven systems [53,54]. The open-source implementation introduced above provides a practical basis for exploring these extensions. We expect this framework to become a practical tool for advancing control techniques in circuit QED platforms.

ACKNOWLEDGMENTS

We acknowledge useful discussions with Göran Johansson, Marina Kudra, and Alberto Del Ángel Medina. All simulations and visualizations were performed using QuTiP [55,56], NumPy [57], and Matplotlib [58]. We acknowledge support from the Knut and Alice Wallenberg Foundation through the Wallenberg Centre for Quantum Technology (WACQT). S.G. acknowledges financial support from the European Research Council (Grant No. 101041744 ESQuAT).

T.A. conceived and planned the project; M.J. developed the theoretical model, performed the simulations, and analyzed the results; K.H. performed the experiments and analyzed the data with input from A.M.E.; S.G. supported the experimental aspects of the work and provided feedback on the manuscript; M.J. and T.A. wrote the manuscript with feedback from all authors; and T.A. supervised the project. External interest disclosure: S.G. is a cofounder and equity holder in Sweden Quantum AB.

DATA AVAILABILITY

Some of the data that support the findings of this study were generated by numerical simulations. The source code and parameters used to generate the simulations is publicly available [29]. Experimental data are not publicly available. The data are available from the authors upon reasonable request.

[1] A. Joshi, K. Noh, and Y. Y. Gao, Quantum information processing with bosonic qubits in circuit QED, Quantum Sci. Technol. **6**, 033001 (2021).

[2] O. Milul, B. Guttel, U. Goldblatt, S. Hazanov, L. M. Joshi, D. Chausovsky, N. Kahn, E. Çiftyürek, F. Lafont, and S. Rosenblum, Superconducting cavity qubit with tens of milliseconds single-photon coherence time, PRX Quantum **4**, 030336 (2023).

[3] A. Krasnok, P. Dhakal, A. Fedorov, P. Frigola, M. Kelly, and S. Kutsaev, Superconducting microwave cavities and qubits for quantum information systemss, Appl. Phys. Rev. **11**, 011302 (2024).

[4] C. Flühmann, T. L. Nguyen, M. Marinelli, V. Negnevitsky, K. Mehta, and J. P. Home, Encoding a qubit in a trapped-ion mechanical oscillator, Nature (London) **566**, 513 (2019).

[5] C. Flühmann and J. P. Home, Direct characteristic-function tomography of quantum states of the trapped-ion motional oscillator, Phys. Rev. Lett. **125**, 043602 (2020).

[6] B. de Neeve, T. L. Nguyen, T. Behrle, and J. P. Home, Error correction of a logical grid state qubit by dissipative pumping, Nat. Phys. **18**, 296 (2022).

[7] P. K. Shandilya, D. P. Lake, M. J. Mitchell, D. D. Sukachev, and P. E. Barclay, Optomechanical interface between telecom photons and spin quantum memory, Nat. Phys. **17**, 1420 (2021).

[8] T. H. Haug, A. Frisk Kockum, and R. Van Laer, Heralding entangled optical photons from a microwave quantum processor, Phys. Rev. Appl. **22**, 034068 (2024).

[9] M. Hofheinz, H. Wang, M. Ansmann, R. C. Bialczak, E. Lucero, M. Neeley, A. D. O'Connell, D. Sank, J. Wenner, J. M. Martinis, and A. N. Cleland, Synthesizing arbitrary quantum states in a superconducting resonator, Nature (London) **459**, 546 (2009).

[10] M. Kudra, M. Kervinen, I. Strandberg, S. Ahmed, M. Scigliuzzo, A. Osman, D. P. Lozano, M. O. Tholén, R. Borgani, D. B. Haviland, G. Ferrini, J. Bylander, A. F. Kockum, F. Quijandría, P. Delsing, and S. Gasparinetti, Robust preparation of Wigner-negative states with optimized SNAP-displacement sequences, PRX Quantum **3**, 030301 (2022).

[11] Z. Ni, S. Li, X. Deng, Y. Cai, L. Zhang, W. Wang, Z.-B. Yang, H. Yu, F. Yan, S. Liu, C.-L. Zou, L. Sun, S.-B. Zheng, Y. Xu, and D. Yu, Beating the break-even point with a discrete-variable-encoded logical qubit, Nature (London) **616**, 56 (2023).

[12] R. W. Heeres, B. Vlastakis, E. Holland, S. Krastanov, V. V. Albert, L. Frunzio, L. Jiang, and R. J. Schoelkopf, Cavity state manipulation using photon-number selective phase gates, Phys. Rev. Lett. **115**, 137002 (2015).

[13] J. M. Gertler, B. Baker, J. Li, S. Shirol, J. Koch, and C. Wang, Protecting a bosonic qubit with autonomous quantum error correction, Nature (London) **590**, 243 (2021).

[14] P. Campagne-Ibarcq, E. Zalys-Geller, A. Narla, S. Shankar, P. Reinhold, L. Burkhart, C. Axline, W. Pfaff, L. Frunzio, R. J. Schoelkopf, and M. H. Devoret, Deterministic remote entanglement of superconducting circuits through microwave two-photon transitions, Phys. Rev. Lett. **120**, 200501 (2018).

[15] M. Kudra, M. Jirlow, M. Kervinen, A. M. Eriksson, F. Quijandría, P. Delsing, T. Abad, and S. Gasparinetti, Experimental realization of deterministic and selective photon

addition in a bosonic mode assisted by an ancillary qubit, Quantum Sci. Technol. **10**, 045037 (2025).
[16] M. Mirrahimi, Z. Leghtas, V. V. Albert, S. Touzard, R. J. Schoelkopf, L. Jiang, and M. H. Devoret, Dynamically protected cat-qubits: A new paradigm for universal quantum computation, New J. Phys. **16**, 045014 (2014).
[17] A. P. Saiko, R. Fedaruk, and S. A. Markevich, Kerr-like nonlinearities in an optomechanical system with an asymmetric anharmonic mechanical resonator, JETP Lett. **113**, 487 (2021).
[18] P. Rabl, Photon blockade effect in optomechanical systems, Phys. Rev. Lett. **107**, 063601 (2011).
[19] A. Nunnenkamp, K. Børkje, and S. M. Girvin, Single-photon optomechanics, Phys. Rev. Lett. **107**, 063602 (2011).
[20] C. Flühmann, V. Negnevitsky, M. Marinelli, and J. P. Home, Sequential modular position and momentum measurements of a trapped ion mechanical oscillator, Phys. Rev. X **8**, 021001 (2018).
[21] K. R. Motes, B. Q. Baragiola, A. Gilchrist, and N. C. Menicucci, Encoding qubits into oscillators with atomic ensembles and squeezed light, Phys. Rev. A **95**, 053819 (2017).
[22] N. Ofek, A. Petrenko, R. Heeres, P. Reinhold, Z. Leghtas, B. Vlastakis, Y. Liu, L. Frunzio, S. M. Girvin, L. Jiang, M. Mirrahimi, M. H. Devoret, and R. J. Schoelkopf, Extending the lifetime of a quantum bit with error correction in superconducting circuits, Nature (London) **536**, 441 (2016).
[23] L. Hu, Y. Ma, W. Cai, X. Mu, Y. Xu, W. Wang, Y. Wu, H. Wang, Y. P. Song, C.-L. Zou, S. M. Girvin, L.-M. Duan, and L. Sun, Quantum error correction and universal gate set operation on a binomial bosonic logical qubit, Nat. Phys. **15**, 503 (2019).
[24] P. Campagne-Ibarcq, A. Eickbusch, S. Touzard, E. Zalys-Geller, N. E. Frattini, V. V. Sivak, P. Reinhold, S. Puri, S. Shankar, R. J. Schoelkopf, L. Frunzio, M. Mirrahimi, and M. H. Devoret, Quantum error correction of a qubit encoded in grid states of an oscillator, Nature (London) **584**, 368 (2020).
[25] A. Grimm, N. E. Frattini, S. Puri, S. O. Mundhada, S. Touzard, M. Mirrahimi, S. M. Girvin, S. Shankar, and M. H. Devoret, Stabilization and operation of a Kerr-cat qubit, Nature (London) **584**, 205 (2020).
[26] W. Cai, Y. Ma, W. Wang, C.-L. Zou, and L. Sun, Bosonic quantum error correction codes in superconducting quantum circuits, Fundam. Res. **1**, 50 (2021).
[27] V. V. Sivak, A. Eickbusch, B. Royer, S. Singh, I. Tsioutsios, S. Ganjam, A. Miano, B. L. Brock, A. Z. Ding, L. Frunzio, S. M. Girvin, R. J. Schoelkopf, and M. H. Devoret, Real-time quantum error correction beyond break-even, Nature (London) **616**, 50 (2023).
[28] D. Lachance-Quirion, M.-A. Lemonde, J. O. Simoneau, L. St-Jean, P. Lemieux, S. Turcotte, W. Wright, A. Lacroix, J. Fréchette-Viens, R. Shillito, F. Hopfmueller, M. Tremblay, N. E. Frattini, J. Camirand Lemyre, and P. St-Jean, Autonomous quantum error correction of Gottesman-Kitaev-Preskill states, Phys. Rev. Lett. **132**, 150607 (2024).
[29] M. Jirlow, martin-jw/late-RWA-Hamiltonian (Version 1.0.0) [Computer software], Zenodo, 2026, https://doi.org/10.5281/zenodo.22304140.
[30] See Supplemental Material at http://link.aps.org/supplemental/10.1103/y7xr-jq5w for system parameters, derivations, and additional simulation results, which includes Refs. [31,32].
[31] M. Malekakhlagh, A. Petrescu, and H. E. Türeci, Lifetime renormalization of weakly anharmonic superconducting qubits. I. Role of number nonconserving terms, Phys. Rev. B **101**, 134509 (2020).
[32] H.-P. Breuer and F. Petruccione, *The Theory of Open Quantum Systems* (Oxford University Press, London, 2002).
[33] B. J. Chapman, S. J. De Graaf, S. H. Xue, Y. Zhang, J. Teoh, J. C. Curtis, T. Tsunoda, A. Eickbusch, A. P. Read, A. Koottandavida, S. O. Mundhada, L. Frunzio, M. H. Devoret, S. M. Girvin, and R. J. Schoelkopf, High-on-off-ratio beamsplitter interaction for gates on bosonically encoded qubits, PRX Quantum **4**, 020355 (2023).
[34] S. Rosenblum, Y. Y. Gao, P. Reinhold, C. Wang, C. J. Axline, L. Frunzio, S. M. Girvin, L. Jiang, M. Mirrahimi, M. H. Devoret, and R. J. Schoelkopf, A CNOT gate between multiphoton qubits encoded in two cavities, Nat. Commun. **9**, 652 (2018).
[35] X. You, Y. Lu, T. Kim, D. M. Kürkçüolu, S. Zhu, D. Van Zanten, T. Roy, Y. Lu, S. Chakram, A. Grassellino, A. Romanenko, J. Koch, and S. Zorzetti, Crosstalk-robust quantum control in multimode bosonic systems, Phys. Rev. Appl. **22**, 044072 (2024).
[36] Y. Y. Gao, B. J. Lester, K. S. Chou, L. Frunzio, M. H. Devoret, L. Jiang, S. M. Girvin, and R. J. Schoelkopf, Entanglement of bosonic modes through an engineered exchange interaction, Nature (London) **566**, 509 (2019).
[37] J. Landgraf, C. Flühmann, T. Fösel, F. Marquardt, and R. J. Schoelkopf, Fast quantum control of cavities using an improved protocol without coherent errors, Phys. Rev. Lett. **133**, 260802 (2024).
[38] S. Li, Z. Ni, L. Zhang, Y. Cai, J. Mai, S. Wen, P. Zheng, X. Deng, S. Liu, *et al.*, Autonomous stabilization of Fock states in an oscillator against multiphoton losses, Phys. Rev. Lett. **132**, 203602 (2024).
[39] S. Shirol, S. van Geldern, H. Xi, and C. Wang, Passive quantum error correction of photon loss at breakeven Phys. Rev. X **16**, 021042 (2026).
[40] C.-H. Wang, K. Noh, J. Lebreuilly, S. M. Girvin, and L. Jiang, Photon-number-dependent Hamiltonian engineering for cavities, Phys. Rev. Appl. **15**, 044026 (2021).
[41] V. Maurya, H. Zhang, D. Kowsari, A. Kuo, D. M. Hartsell, C. Miyamoto, J. Liu, S. Shanto, E. Vlachos, A. Zarassi, K. W. Murch, and E. M. Levenson-Falk, On-demand driven dissipation for cavity reset and cooling, PRX Quantum **5**, 020321 (2024).
[42] Y. Zhang, J. C. Curtis, C. S. Wang, R. J. Schoelkopf, and S. M. Girvin, Drive-induced nonlinearities of cavity modes coupled to a transmon ancilla, Phys. Rev. A **105**, 022423 (2022).
[43] J. Huang, T. J. DiNapoli, G. Rockwood, M. Yuan, P. Narasimhan, E. Gupta, M. Bal, F. Crisa, S. Garattoni, Y. Lu, L. Jiang, and S. Chakram, Fast sideband control of a multimode cavity memory with weak dispersive coupling to a transmon, Phys. Rev. X **16**, 011058 (2026).
[44] J. Koch, V. Manucharyan, M. H. Devoret, and L. I. Glazman, Charging effects in the inductively shunted Josephson junction, Phys. Rev. Lett. **103**, 217004 (2009).
[45] V. E. Manucharyan, J. Koch, L. I. Glazman, and M. H. Devoret, Fluxonium: Single Cooper-pair circuit free of charge offsets, Science **326**, 113 (2009).
[46] L. B. Nguyen, Y.-H. Lin, A. Somoroff, R. Mencia, N. Grabon, and V. E. Manucharyan, High-coherence fluxonium qubit, Phys. Rev. X **9**, 041041 (2019).

[47] K. Nie, J. N. Bradford, S. Mandal, A. Bista, W. Pfaff, and A. Kou, Fluxonium as a control qubit for bosonic quantum information, PRX Quantum **7**, 010357 (2026).

[48] J. M. Martinis, Superconducting phase qubits, Quantum Inf. Process. **8**, 81 (2009).

[49] T. P. Orlando, J. E. Mooij, L. Tian, C. van der Wal, L. Levitov, S. Lloyd, and J. J. Mazo, Superconducting persistent-current qubit, Phys. Rev. B **60**, 15398 (1999).

[50] J. E. Mooij, T. P. Orlando, L. Levitov, L. Tian, C. H. van der Wal, and S. Lloyd, Josephson persistent-current qubit, Science **285**, 1036 (1999).

[51] J. Koch, T. M. Yu, J. Gambetta, A. A. Houck, D. I. Schuster, J. Majer, A. Blais, M. H. Devoret, S. M. Girvin, and R. J. Schoelkopf, Charge-insensitive qubit design derived from the Cooper pair box, Phys. Rev. A **76**, 042319 (2007).

[52] P. Magnard, P. Kurpiers, B. Royer, T. Walter, J.-C. Besse, S. Gasparinetti, M. Pechal, J. Heinsoo, S. Storz, A. Blais, and A. Wallraff, Fast and unconditional all-microwave reset of a superconducting qubit, Phys. Rev. Lett. **121**, 060502 (2018).

[53] J. Yang, M. Khanahmadi, I. Strandberg, A. Gaikwad, C. Castillo-Moreno, A. Frisk Kockum, M. A. Ullah, G. Johansson, A. M. Eriksson, and S. Gasparinetti, Deterministic generation of frequency-bin-encoded microwave photons, Phys. Rev. Lett. **134**, 240803 (2025).

[54] J. Yang, A. M. Eriksson, M. A. Aamir, I. Strandberg, C. Castillo-Moreno, D. Perez Lozano, P. Persson, and S. Gasparinetti, Deterministic generation of shaped single microwave photons using a parametrically driven coupler, Phys. Rev. Appl. **20**, 054018 (2023).

[55] J. R. Johansson, P. D. Nation, and F. Nori, QuTiP: An open-source Python framework for the dynamics of open quantum systems, Comput. Phys. Commun. **183**, 1760 (2012).

[56] J. R. Johansson, P. D. Nation, and F. Nori, QuTiP 2: A Python framework for the dynamics of open quantum systems, Comput. Phys. Commun. **184**, 1234 (2013).

[57] C. R. Harris, K. J. Millman, S. J. Van Der Walt, R. Gommers, P. Virtanen, D. Cournapeau, E. Wieser, J. Taylor, S. Berg, N. J. Smith, R. Kern, M. Picus, S. Hoyer, M. H. Van Kerkwijk, M. Brett, A. Haldane, J. F. Del Río, M. Wiebe, P. Peterson, P. Gérard-Marchant, *et al.*, Array programming with NumPy, Nature (London) **585**, 357 (2020).

[58] J. D. Hunter, Matplotlib: A 2D graphics environment, Comput. Sci. Eng. **9**, 90 (2007).